IOP Conf. Series: Journal of Physics: Conf. Series **1455** (2020) 012030 doi:10.1088/1742-6596/1455/1/012030

Comparative studies on the corrosion behavior of some Zr-based amorphous alloys having different compositions in nitric acid medium

Poonam Sharma[1], Anil Dhawan[1,*], and S. K. Sharma[2]

[1]Department of Physics, Anand International College of Engineering, Jaipur-303012, India
[2]Department of Physics, Malaviya National Institute of Technology, Jaipur-302017, India

dr.anildhawan11@gmail.com +91 9829276707)

Abstract—The corrosion studies were performed on different composition of Zr-based bulk amorphous ribbon alloys such as $Zr_{55}Cu_{30}Ni_5Al_{10}$, $Zr_{60}Nb_2Cu_{20}Ni_8Al_{10}$, $Zr_{59}Nb_3Cu_{20}Ni_8Al_{10}$, $Zr_{57}Nb_5Cu_{20}Ni_8Al_{10}$ and $Zr_{60}Pd_5Cu_{15}Ni_{10}Al_{10}$ alloys at room temperature. The amorphous nature of all the above mentioned alloys was confirmed by X-ray diffraction (XRD). The corrosion behavior was investigated using potentiodynamic polarization and weight loss analysis methods at room temperature. Surface morphology of these corroded samples were investigated by optical microscopy and scanning electron microscopy (SEM). The results of the investigations revealed the fact that Nb containing Zr-based bulk amorphous alloys shows better corrosion resistance among all the investigated alloys due to the presence of Nb_2O_5. The presence of Nb_2O_5 on the surface of Nb containing Zr-based bulk amorphous alloy after immersion in HNO_3 medium was confirmed by X-ray photoelectron spectroscopy (XPS) techniques.
*Keywords—*Amorphous alloys, Corrosion, SEM, XPS.

1. INTRODUCTION

BULK metallic glasses generally exhibit outstanding mechanical properties such as high mechanical strength, high fracture toughness and good corrosion resistance which cannot be obtained for conventional materials [1]. Among glass forming systems, Zr-based multi-component alloys have received more attention due to the easy castability and high thermal stability against crystallization together with interesting mechanical properties [2], [3]. Environmental degradation pertains to the study of oxidation and corrosion behavior of the amorphous alloy in terms of its utility and various engineering applications. In order to investigate the performance of highly corrosion resistant amorphous alloy, electrochemical investigations were carried out on Zr-based amorphous alloys by many researchers such as Dhawan et al. [4] in aqueous HNO_3 solutions, Raju et al. [5] in Na_2SO_4 and NaCl, S. Pang et al [6] in HCl, NaCl and H_2SO_4 solutions and Qin et al. [7] in NaCl medium.The interest for the present investigation resulted primarily from the lack of sufficient data in the literature on the corrosion behaviour of the Zr-based bulk amorphous alloys in different concentration of nitric acid.

The motivation for the present study was derived from the need of searching a high corrosion resistant glassy alloy in nitric acid environment for various engineering applications. Therefore the main motive of this work is to analyze the corrosion resistance of different Zr-based bulk amorphous alloys using weigh loss analysis methods in 1 M HNO_3, 6 M HNO_3 and 11.5 M HNO_3 medium at room temperature. Detailed surface characterization has been carried out using XRD, SEM and XPS techniques.

I. Experimental Procedure

A. Materials and Micro- structural Characterization

As-received glassy ribbons of $Zr_{55}Cu_{30}Ni_5Al_{10}$, $Zr_{60}Nb_2Cu_{20}Ni_8Al_{10}$, $Zr_{59}Nb_3Cu_{20}Ni_8Al_{10}$, $Zr_{57}Nb_5Cu_{20}Ni_8Al_{10}$ and $Zr_{60}Pd_5Cu_{15}Ni_{10}Al_{10}$ of dimensions 3 mm x 30 μm were used for the investigation. Amorphous nature of the Zr-based amorphous alloy was characterized by XRD technique.

B. Weight Loss Analysis

As-spun ribbon specimens of Zr-based amorphous alloys were cut in same size and were cleanedwith distilled water, acetone and dried in air. The surface area and initial mass of each sample were measured and the samples were thenimmersed in the aqueous medium at room temperature. Each sample was weighed after immersion in the solution for 480 h. The microgram balance (Mettler Toledo) used to measure the actual weight loss of the samples has an accuracy of ±10 µg. Equation (1) is used to determine the corrosion rates [8]:

$$CR(mm/y) = 87.6\frac{W}{DAT} \quad (1)$$

Where, W is weight loss in mg, D is density of the material in g/cm^3 and A is area of the sample exposed to the corrosive environment in inches.

C. Surface Morphology

The surface morphology of the virgin and treated samples was investigated using optical microscope (Radical Universal Trinocular Metallurgical – RMM-8TCE), scanning electron microscope (ZEISS-EVO 18). The chemical composition of the treated samples was investigated by XPS using ESCA+ Omicron Nanotechnology (Oxford Instrument, Germany) at MRC MNIT, Jaipur.

1. Results and Discussion

Micro-structural Characterization

Fig. 1 (a) is XRD pattern of $Zr_{60}Nb_2Cu_{20}Ni_8Al_{10}$, $Zr_{59}Nb_3Cu_{20}Ni_8Al_{10}$, $Zr_{57}Nb_5Cu_{20}Ni_8Al_{10}$ and $Zr_{60}Pd_5Cu_{15}Ni_{10}Al_{10}$ alloys which was recorded by Xpert Pro- Pananalytical system using Cu-Kα radiations whereas the XRD pattern of as-spun $Zr_{55}Cu_{30}Ni_5Al_{10}$ ribbon alloy (fig. 1 (b)) was recorded by Inel-XRD (Equinox 2000) system using monochromatic Co source. Fig. 1 (a) indicates that the typical broad maxima were especially pronounced in the range from 32˚ to 45˚, suggesting that the Zr-based bulk amorphous alloys are predominantly amorphous. Similarly fig. 1 (b) also exhibits the broad maxima in the range from 35˚ to 50˚. No significant peaks corresponding to crystalline phases were identified. These XRD patterns revealed the amorphous nature of the all samples.

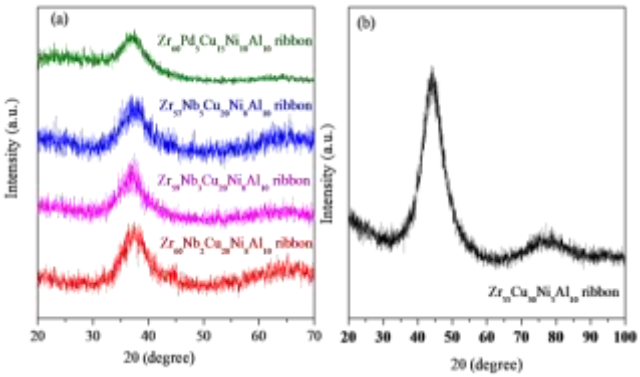

Fig. 1 XRD pattern of (a) different composition of Zr-based ribbon alloys using Cu-Kα radiations; (b) $Zr_{55}Cu_{30}Ni_5Al_{10}$ amorphous ribbon using Co-Kα radiations

Weight Loss Analysis

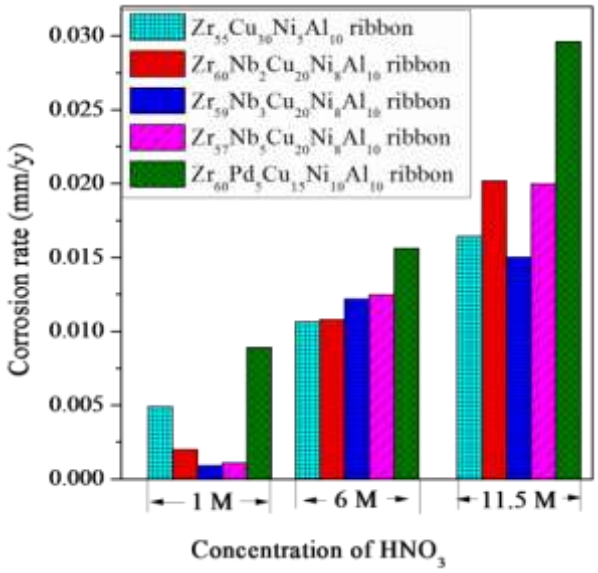

Fig. 2 Corrosion rate versus concentration of HNO_3 plot of different as-spun Zr-based bulk amorphous ribbon alloys exposed in different concentration of nitric acid medium at room temperature for 480 h duration

The corrosion rate of as-spun $Zr_{55}Cu_{30}Ni_5Al_{10}$, $Zr_{60}Nb_2Cu_{20}Ni_8Al_{10}$, $Zr_{59}Nb_3Cu_{20}Ni_8Al_{10}$, $Zr_{57}Nb_5Cu_{20}Ni_8Al_{10}$ and $Zr_{60}Pd_5Cu_{15}Ni_{10}Al_{10}$amorphous ribbon alloys was calculated using weight loss method in various concentration of nitric acid. The plot of the corrosion rates versus concentration of nitric acid of these Zr-based amorphous ribbon alloys at room temperature is shown in fig. 2. The as-spun $Zr_{60}Pd_5Cu_{15}Ni_{10}Al_{10}$ amorphous alloy shows the highest corrosion rate in all concentrations of nitric acid among all the investigated Zr-based amorphous alloys. Fig. 2 revealed that the corrosion rate of all investigated Zr-based amorphous alloys increases with the increase in concentration of HNO_3. It is noticeable from fig. 2 that the Nb containing Zr-based amorphous alloy shows better corrosion resistance in all concentration of nitric acid than $Zr_{60}Pd_5Cu_{15}Ni_{10}Al_{10}$and $Zr_{55}Cu_{30}Ni_5Al_{10}$amorphous alloy. In 11.5 M HNO_3 solution $Zr_{59}Nb_3Cu_{20}Ni_8Al_{10}$ amorphous alloy shows least value of corrosion rate which is significantly less than other alloys. Infact $Zr_{59}Nb_3Cu_{20}Ni_8Al_{10}$ amorphous ribbon alloy exhibits better corrosion resistance in nitric acid environment among all investigated Zr-based amorphous alloys. In the present study, at higher concentration of HNO_3 medium, a significant decrease in corrosion rate has been observed due to the formation of passive layer of niobium oxide.

Surface Morphology

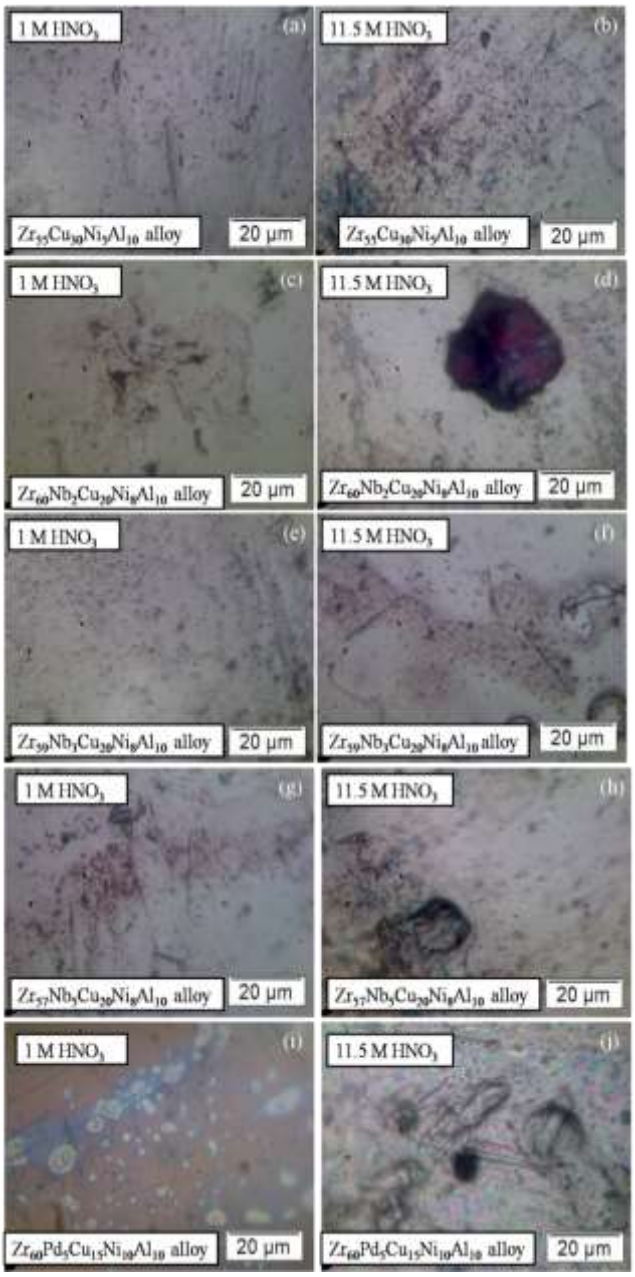

Fig. 3 Optical micrographs of Zr-based bulk amorphous alloys after immersion in different concentration of nitric acid medium for 480 hr at room temperature

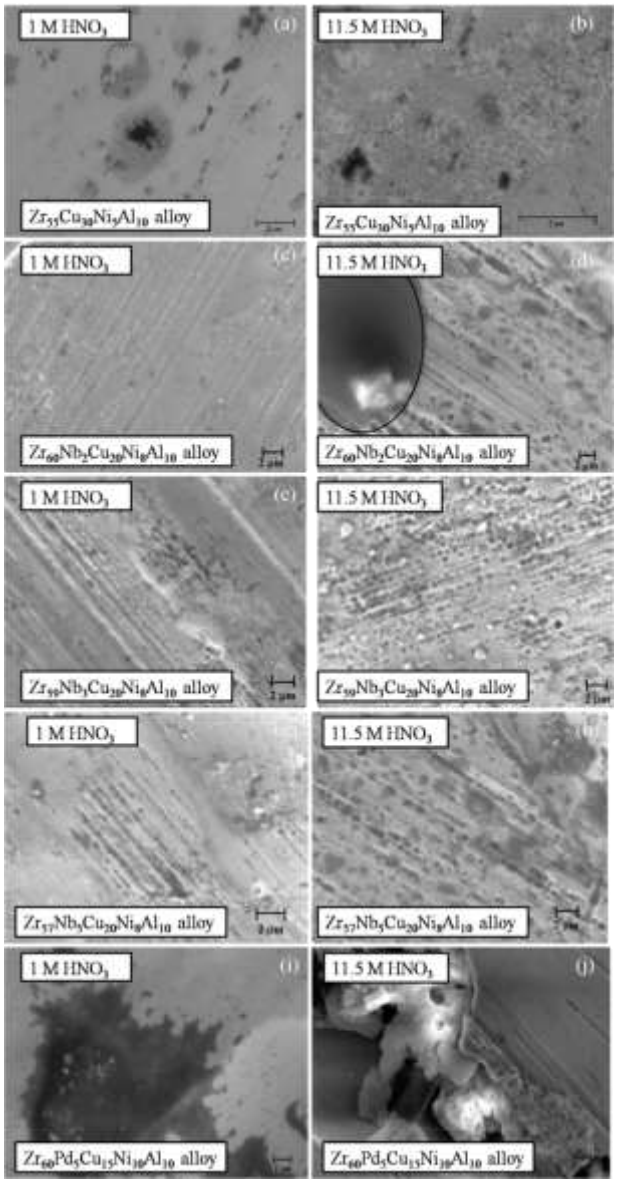

Fig. 4 SEM micrographs of Zr-based bulk amorphous alloys after immersion in different concentration of nitric acid medium for 480 hr at room temperature

The surface morphology of the Zr-based amorphous ribbon alloys after immersion in nitric acid medium were examined by optical microscopy and scanning electron microscopy. Fig. 3 shows the optical micrographs of $Zr_{55}Cu_{30}Ni_5Al_{10}$, $Zr_{60}Nb_2Cu_{20}Ni_8Al_{10}$, $Zr_{59}Nb_3Cu_{20}Ni_8Al_{10}$, $Zr_{57}Nb_5Cu_{20}Ni_8Al_{10}$ and $Zr_{60}Pd_5Cu_{15}Ni_{10}Al_{10}$ amorphous ribbon alloys after immersion in 1 M and 11.5 M aqueous HNO_3 medium for 480 hr at room temperature. Fig. 3 revealed that $Zr_{59}Nb_3Cu_{20}Ni_8Al_{10}$ amorphous alloy possesses better corrosion resistance among all investigated Zr-based bulk amorphous alloys. The optical micrograph of $Zr_{60}Nb_2Cu_{20}Ni_8Al_{10}$and $Zr_{59}Nb_3Cu_{20}Ni_8Al_{10}$ amorphous alloys exhibit the presence of passive layer on the surface of immersed sample in 1 M and 11.5 M HNO_3 solution. These results revealed that the surface of $Zr_{57}Nb_5Cu_{20}Ni_8Al_{10}$ amorphous alloy immersed in 1 M HNO_3 (fig.3 (g)) and 11.5 M HNO_3 (fig. 3 (h)) was profoundly corroded than the surface of $Zr_{60}Nb_2Cu_{20}Ni_8Al_{10}$and $Zr_{59}Nb_3Cu_{20}Ni_8Al_{10}$ amorphous alloys. On the other hand, $Zr_{60}Pd_5Cu_{15}Ni_{10}Al_{10}$ amorphous alloy was severly corroded among all investigated Zr-based bulk amorphous alloys as shown in optical micrographs (fig. 3 (i) and 3 (j)). Fig. 4 exhibits theSEM micrographs of $Zr_{55}Cu_{30}Ni_5Al_{10}$, $Zr_{60}Nb_2Cu_{20}Ni_8Al_{10}$, $Zr_{59}Nb_3Cu_{20}Ni_8Al_{10}$, $Zr_{57}Nb_5Cu_{20}Ni_8Al_{10}$ and $Zr_{60}Pd_5Cu_{15}Ni_{10}Al_{10}$ amorphous ribbon alloys after immersion in 1 M aqueous HNO_3 and 11.5 M aqueous HNO_3 medium for 480 hr. The SEM micrographs revealed that the $Zr_{59}Nb_3Cu_{20}Ni_8Al_{10}$ glassy alloy shows clean surface (fig. 4 (e) and (f)) as compared to all other investigated alloys in 1 M and 11.5 M HNO_3 medium. The formation

of oxide pockets were observed on the surface of $Zr_{59}Nb_3Cu_{20}Ni_8Al_{10}$ amorphous alloy after immersion in 11.5 M HNO_3 medium as shown in fig. 4(f). SEM results exhibit that the $Zr_{55}Cu_{30}Ni_5Al_{10}$ (fig. 4 (a) and (b)) and $Zr_{60}Pd_5Cu_{15}Ni_{10}Al_{10}$ (fig. 4 (i) and (j)) amorphous alloys were severely corroded in nitric acid medium. SEM results indicate the possibility of pilling off of the passive film formed on the $Zr_{60}Nb_2Cu_{20}Ni_8Al_{10}$ alloy at 11.5 M HNO_3, as shown in fig. 4 (d). These optical and SEM results were in good agreement with results of weight loss analysis.

XPS Study

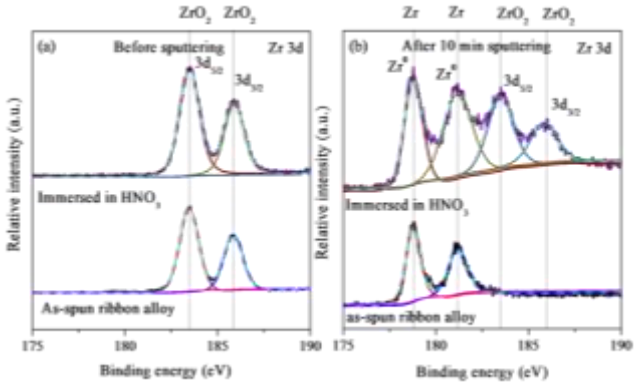

Fig. 5 High resolution XPS spectra of Zr for as-spun and immersed $Zr_{59}Nb_3Cu_{20}Ni_8Al_{10}$ amorphous alloy in 11.5 M HNO_3 medium for 480 hours (a) before sputtering and (b) after 10 min sputtering

To understand the compositional changes on the surface of $Zr_{59}Nb_3Cu_{20}Ni_8Al_{10}$ amorphous alloy after immersion in 11.5 M HNO_3 medium, XPS studies were carried out on as-spun and immersed sample. The high-resolution XPS spectra of Zr and Nb for as-spun and immersed $Zr_{59}Nb_3Cu_{20}Ni_8Al_{10}$ amorphous alloy in 11.5 M HNO_3 for 480 hours, before and after sputtering of 10 minutes, are shown in fig. 5 and 6, respectively. The fig. 5 (a) represents the Zr 3d spectra of as-spun and immersed $Zr_{59}Nb_3Cu_{20}Ni_8Al_{10}$ amorphous alloy before sputtering and fig. 5 (b) shows the Zr 3d spectra of as-spun and immersed $Zr_{59}Nb_3Cu_{20}Ni_8Al_{10}$ amorphous alloy after 10 minutes sputtering. The deconvolution of Zr 3d spectra was done in the terms of metal Zr^0 and oxide ZrO_2 based on the literature values of their binding energies. The peaks of ZrO_2 were observed at the binding energies 183.3 eV and 185.7 eV corresponding to the peaks of $Zr3d_{5/2}$ and Zr $3d_{3/2,}$ respectively [9], [10].These peaks corresponding to ZrO_2 were observed before sputtering of the sample in both the conditions of sample i.e. surface of as-spun alloy and after immersion in nitric acid medium. The intensity of XPS peaks corresponding to ZrO_2 was high in the case of immersed sample. The peaks at 179.3 eV and 181.7 eV corresponding to metallic Zr [11] were observed after 10 min of sputtering along with peak corresponding to Zr^{4+} for as-spun alloy. However, the immersed sample has shown the presence of ZrO_2 along with metallic Zr after 10 min sputtering of the sample. The presence of ZrO_2 on the surface of as-cast sample was due to the formation of native oxide, which could not be observed after 10 min of sputtering.

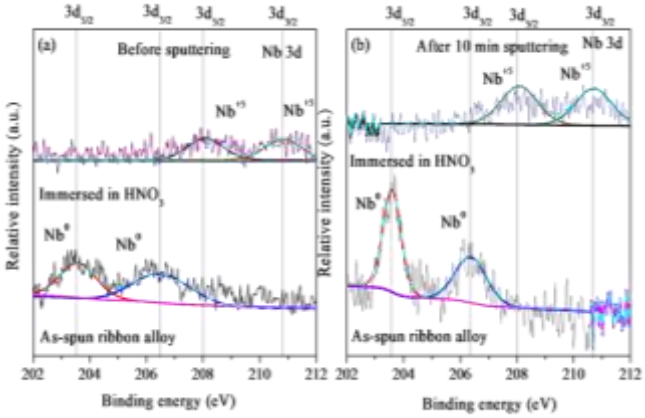

Fig. 6 High resolution XPS spectra of Nb for as-spun and immersed $Zr_{59}Nb_3Cu_{20}Ni_8Al_{10}$ amorphous alloy in 11.5 M HNO_3 medium for 480 hours (a) before

sputtering and (b) after 10 min sputtering

The surface of as-spun sample exhibited the presence of Nb^0 peak corresponding to metallic Nb at 203.6 eV and 206.4 eV binding energy, as shown in fig. 6 (a) [12], but the surface of immersed sample clearly exhibited the presence of XPS peaks corresponding to the Nb^{5+} state at 208.0 and 210.7 eV (fig. 6 (a)), respectively which are assigned to Nb_2O_5 [12]. No peak corresponding to metallic Nb could be observed on the surface of $Zr_{59}Nb_3Cu_{20}Ni_8Al_{10}$ amorphous alloy after immersion in 11.5 M HNO_3 medium. Fig. 6 (b) revealed that the as-spun alloy shows the presence of metallic Nb after 10 min of sputtering, whereas the immersed sample exhibits the XPS peaks corresponding to Nb^{+5} state indicating the presence of Nb_2O_5 after 10 min of sputtering.

These XPS results revealed the fact that the formation of passive film of ZrO_2, Al_2O_3 and Nb_2O_5 take place on the surface of $Zr_{59}Nb_3Cu_{20}Ni_8Al_{10}$ amorphous alloy after immersion in HNO_3 medium. Since ZrO_2 layer has a strong passivation ability and high corrosion resistance in H^+-containing solutions [13] thus, it protects the alloy from corrosion. Also, Nb_2O_5 possesses corrosion resistant properties [14] hence it is useful in protecting the alloy from corrosion attack in aqueous solutions.

Conclusions

The corrosion behavior of Zr-based amorphous alloys such as $Zr_{55}Cu_{30}Ni_5Al_{10}$, $Zr_{60}Nb_2Cu_{20}Ni_8Al_{10}$, $Zr_{59}Nb_3Cu_{20}Ni_8Al_{10}$, $Zr_{57}Nb_5Cu_{20}Ni_8Al_{10}$ and $Zr_{60}Pd_5Cu_{15}Ni_{10}Al_{10}$ alloys in 1 M HNO_3, 6 M HNO_3 and 11.5 M HNO_3 concentration of nitric acid medium has been investigated by weight loss analysis. It is concluded from above mentioned investigations that Nb-containing Zr-based amorphous alloys possesses better corrosion resistance among all investigated alloys. The better corrosion resistance of Nb-containing Zr-based bulk amorphous alloys was attributed to the formation of passive layer containing ZrO_2 and Nb_2O_5 which was confirmed by XPS study.

ACKNOWLEDGMENT

The financial support for this work under BRNS/DAE, Govt. of India, Research Project No. 2011/36/44-BRNS/1974 is gratefully acknowledged. We are thankful to Dr. U. K. Mudali, IGCAR Kalpakkam for providing the samples. We are also thankful to MRC, Malaviya National Institute of Technology, Jaipur for the XPS facility and USIC, Department of Physics, University of Rajasthan, Jaipur for SEM Facility.

REFERENCES

[1] A. Inoue, "Bulk amorphous alloys", Pergamon Material Series, vol. 2, pp. 375-415, 1999, Ch. 14.
[2] A. Inoue, "Stabilization of Metallic Supercooled Liquid and Bulk Amorphous Alloys", Acta Mater., vol. 48, no. 1, pp. 279-306, Jan. 2000.
[3] A. Inoue, "Bulk Amorphous And Nanocrystalline Alloys with High Functional Properties", Mater. Sci. Eng. A, vol. 304–306, pp. 1–10, May 2001.
[4] A. Dhawan, K. Sachdev, S. Roychowdhury, P. K. De, and S. K. Sharma, "Potentiodynamic Polarization Studies in Amorphous $Zr_{46.75}Ti_{8.25}Cu_{7.5}Ni_{10}Be_{27.5}$, $Zr_{65}Ni_{10}Cu_{17.5}Al_{7.5}$, $Zr_{67}Ni_{33}$ And $Ti_{60}Ni_{40}$ in Aqueous HNO_3 Solution", J. Non-Cryst. Solids, vol. 353, pp. 2619-2623, Aug. 2007.
[5] V. R. Raju, U. Kuhn, U. Wolff, F. Schneider, J. Eckert, R. Reiche and A. Gebert, "Corrosion Behaviour of Zr-Based Bulk Glass-Forming Alloys Containing Nb or Ti", Mater. Lett., vol. 57, pp. 173-177, Nov. 2002.
[6] S. Pang, T. Zhang, H. Kimura, K. Asami and A. Inoue, "Corrosion Behaviour of Zr-(Nb)-Al-Ni-Cu Glassy Alloy", Mater. Trans. JIM, vol. 41, pp. 1490-1494, June 2000.
[7] F. X. Qin, H. F. Zhang, Y. F. Deng, B. Z. Ding, and , Z. Q. Hu, "Corrosion Resistance of Zr-Based Bulk Amorphous Alloys Containing Pd", J. Alloys Compd., vol. 375, pp. 318-323, July 2004.
[8] M.G Fontana, "Corrosion Testing", in Corrosion Engineering,3rd Edn, Ed. New York: Tata Mc. Graw-Hill, 2005.
[9] S. K. Sharma, T. Strunskus, H. Ladebusch, and F. Faupel "Surface Oxidation of Amorphous Zr65Cu17.5Ni10Al7.5 and Zr46.75Ti8.25Cu7.5Ni10Be27.5", Mater. Sci. Eng. A, vol. 304-306, pp. 747-752, May 2001.
[10] R. Kaufmann, H. Klewe-Nebenius, H. Moers, G. Pfennig, H. Jenett and H. J. Ache, "XPS Studies of the Thermal Behaviour of Passivated Zircaloy-4 Surfaces", Surf. Interface. Anal.,vol.11, pp. 502-509, July 1988.
[11] X. P. Nie, X. H. Yang, L. Y. Chen, K. B. Yeap, K. Y. Zeng, D. Li, J. S. Pan, X. D. Wang, Q. P. Cao, S. Q. Ding and J. Z. Jiang, "The Effect of Oxidation on the Corrosion Resistance and Mechanical Properties of a Zr-Based Metallic Glass", Corros. Sci.,vol. 53, pp. 3557–3565, Nov. 2011.
[12] C. Qin, K. Asami, H. Kimura, W. Zhang and A. Inoue, "Electrochemical and XPS Studies of Ni-Based Metallic Glasses in Boiling Nitric Acid Solutions", Electrochimica Acta., vol. 54, pp. 1612-1617, Feb. 2009.
[13] B. Lustman and F. Kerze, "The Metallurgy of Zirconium", Jr. (eds.) Ed. New York: Mc Graw Hill, USA 1955.
[14] R. Mythili, S. Saroja and M. Vijayalakshmi, "Characterization of Passive Oxide Film on a Ti–5%Ta–1.8%Nb Alloy on Exposure to Severe Oxidizing Conditions", Mater Charact., vol. 61, pp. 1326 – 1334, Dec. 2010.